2023 IEEE 24th International Workshop on Signal Processing Advances in Wireless Communications (SPAWC) | 978-1-6654-9626-1/23/$31.00 ©2023 IEEE | DOI: 10.1109/SPAWC53906.2023.10304433

Learning based Compressive Beam Detection Using Real-valued Beamspace Covariance Processing for mmWave Communications

Zhibin Yu * Ahmed Abdelkader* Xiaofeng Wu * Martin Haardt †
* Munich Research Center, Huawei Technologies Duesseldorf GmbH, Munich, Germany
† Communications Research Lab, Ilmenau University of Technology, Ilmenau, Germany
* Email: {zhibinyu,ahmed.abdelkader3,xiaofeng.wu1}@huawei.com
† Email: {martin.haardt}@tu-ilmenau.de

***Abstract*—In this paper, we present a learning based beam detection scheme using compressive measurements in mmWave band communications. By considering that the measured beamspace covariance (BSC) is the compressive projection of the antenna-element-space covariance (AESC) of the spatial channel, while the latter is directly associated to the optimal communication beam, the upper triangular part of the BSC matrix is selected as the input feature of a feed-forward neural network (NN) which directly detects the best communication beam. We also show that, by designing the training beams with structured random phases to be conjugate symmetric, the real part of the BSC becomes the compressive projection of the forward-backward (FB) averaged version of the AESC. This property leads to a small real-valued NN with less nodes. Simulations show that the proposed scheme outperforms the traditional two-step approach, with only a few measurements.**

***Index Terms*—compressive beam detection, training codebook design, beamspace spatial covariance, deep learning.**

I. Introduction

The millimeter wave (mmWave) band provides a wide bandwidth for high data throughput and has been adopted by 5G new radio (NR) cellular communication systems. To overcome the high path-loss through mmWave band propagation while at the same time being cost efficient and power efficient, large antenna arrays based on analog beamforming with phase shifters have become a popular architecture not only on the base station (BS) side but also on the user equipment (UE) side. To ensure reliable communication, beam training is required to detect the best communication beam pairs before the data communication link is set up. However, due to the sharing of the RF chains among multiple antenna elements, the baseband processor does not directly observe the channel state information (CSI) in the antenna element space, but rather the projected version in the beamspace. This leads to challenges for coherent beam training [1].

By exploring the sparsity of the mmWave propagation channel, compressive sensing (CS) techniques can be explored to estimate the CSI in the antenna element space using a small training overhead. Several CS based spatial channel estimation algorithms for OFDM have been proposed and compared by [2], which shows that the spatial channel transfer function in the antenna element space can be recovered through compressive measurements using random training beams. An off-grid refinement method on top of the on-grid recovery has been proposed by [3], which can estimate the directions of arrival (DoAs) with high resolution using compressive measurements. Instead of using fully randomized training beams, [4] proposes to use structured random training beams for compressive measurements, so that the spatial channel recovery can be robust against phase errors during time multiplexed measurements. Compressive recovery in the covariance domain has been proposed by [5], wherein the antenna element space covariance (AESC) of the spatial channel can be on-grid recovered from the measured beamspace covariance (BSC), through a covariance orthogonal matching pursuit (COMP) algorithm.

By considering that the compressive recovery is non-linear, machine learning tools are also explored to solve the beam detection problem for mmWave communications. The authors of [6] and [7] have proposed to feed the raw measurement IQ samples into a pre-trained convolutional neural network (CNN) to directly classify the optimal beam index. Since the raw measurement IQ data is directly fed into the NN, heavy convolutional layers are required to compress the features. The authors of [8] and [9], on the other hand, have proposed to feed the measurement power, as phase-less features, into the neural network for beam classification. Since the phase information is totally dropped, heavy convolutional layers as well as wide dense layers are again required to expand the implicit features, which is computationally expensive.

Inspired by [5], we propose to apply compressive recovery in the covariance domain. However, instead of first applying on-grid compressive recovery of the AESC and then use it to detect the best communication beam, we treat the upper triangular part of the BSC matrix as the compressed features associated to the spatial channel, and feed them into a feed-forward neural network (NN) to predict the beamforming gains of the candidate communication beams. This gives the benefits that the grid-mismatch issue can be mitigated by the neural network. We also propose that, by introducing structured random training beams which are conjugate symmetric, the real part of the BSC is a compressive projection of the forward-backward (FB) version of AESC. Those result in a small real-valued NN with only a few nodes. Simulation results show that the proposed scheme outperforms the two step approach and can reliably detect the best communication beam using only few measurements.

Notation: Upper-case and lower-case bold-faced letters denote matrices and vectors, respectively. The expectation, transpose, conjugate, Hermitian transpose, floor operation are denoted by $\mathbb{E}\{.\}, \{\}^T, \{\}^*, \{\}^H, \lfloor . \rfloor$, respectively. The element in i^{th} row and j^{th} column of matrix $\mathbf{A}$ is denoted as $[\mathbf{A}]_{i,j}$ and $\mathbf{I}_N$ denotes $N \times N$ identity matrix.

II. Problem Formulation

A. System Model

We consider a typical mmWave MIMO communication system with a base station (BS) and a user equipment (UE) both equipped with T and N antennas, respectively. The antennas on both sides are assumed to form a Uniform-Linear Arrays (ULA) which uses phase shifters for transmit and receive signal beamforming.

During the downlink transmission, the BS transmits a training burst of M OFDM symbols each containing K pilot reference sub-carriers. The pilot symbols are mapped to the same OFDM sub-carriers in all M symbols and are used at the UE side to perform receive beam training. We assume that the transmit beam at the BS is fixed during the training burst whereas, the UE uses M different training beams to receive the M OFDM symbols where $M \ll N$. The switching time from one training beam to the next is assumed to be shorter than the CP duration. We further assume that all M OFDM symbols are transmitted within the channel coherence time so that the channel could be assumed to be constant during the training. On the receiver side, after applying the FFT operation for the m^{th} received OFDM symbol, the frequency domain received signal on k^{th} sub-carrier is formulated as:

$$y_m(k) = \mathbf{w}_m^H \mathbf{H}(k) \mathbf{f} s_m(k) + \mathbf{w}_m^H \mathbf{z}_m(k) \tag{1}$$

where $\mathbf{z}_m(k) \in \mathbb{C}^{N\times 1}$ is a zero mean complex Gaussian noise vector with variance σ^2, $s_m(k)$ is the pilot reference signal on the k^{th} sub-carrier of the m^{th} OFDM symbol and $|s_m(k)| = 1$. Moreover, $\mathbf{f} \in \mathbb{C}^{T\times 1}$ is the vector of beamforming coefficients at the BS which is fixed over the training burst while $\mathbf{w}_m \in \mathbb{C}^{N\times 1}$ is the receive beamforming vector at the UE for the m^{th} OFDM symbol. Since the beams are formed by using analog phase shifters, $\mathbf{f}$ and $\mathbf{w}_m$ contain only unit modulus entries. The matrix $\mathbf{H}(k) \in \mathbb{C}^{N\times T}$ is the sampled frequency domain channel transfer function (CTF) on the k^{th} sub-carrier.

A typical mmWave massive MIMO channel is assumed with L scatterers. Each scatterer corresponds to a single propagation path between the BS and the UE, which accounts for one time delay τ_l, one complex gain α_l, and one pair of spatial frequencies $(\mu_{T,l}, \mu_{R,l})$ for $l \in 0, \ldots, L-1$. Then the sampled frequency domain CTF on the k^{th} sub-carrier can be modeled as [10]:

$$\mathbf{H}(k) = \sum_{l=0}^{L-1} \alpha_l e^{-j2\pi k \Delta f \tau_l} \mathbf{a}_R(\mu_{R,l}) \mathbf{a}_T^T(\mu_{T,l}) \tag{2}$$

where Δf is the OFDM sub-carrier spacing, $\mathbf{a}_R(\mu_{R,l}) \in \mathbb{C}^{N\times 1}$ and $\mathbf{a}_T^T(\mu_{T,l}) \in \mathbb{C}^{T\times 1}$ are array steering vectors at the BS and UE side corresponding to l^{th} path and can be written as:

$$\begin{aligned} \mathbf{a}_R(\mu_{R,l}) &= [1, e^{j\mu_{R,l}}, \cdots, e^{j(N-1)\mu_{R,l}}]^T \\ \mathbf{a}_T(\mu_{T,l}) &= [1, e^{j\mu_{T,l}}, \cdots, e^{j(T-1)\mu_{T,l}}]^T. \end{aligned} \tag{3}$$

Since the transmit beamforming vector $\mathbf{f}$ is fixed for all m OFDM symbols, (1) can be written as:

$$y_m(k) = \mathbf{w}_m^H \mathbf{h}(k) s_m(k) + \mathbf{w}_m^H \mathbf{z}_m(k) \tag{4}$$

where

$$\begin{aligned} \mathbf{h}(k) &= \mathbf{H}(k)\mathbf{f} \\ &= \sum_{l=0}^{L-1} \alpha_l e^{-j2\pi k \Delta f \tau_l} \mathbf{a}_R(\mu_{R,l}) \mathbf{a}_T^T(\mu_{T,l}) \mathbf{f} \\ &= \sum_{l=0}^{L-1} \alpha_{R,l}(k) \mathbf{a}_R(\mu_{R,l}) \end{aligned} \tag{5}$$

and $\alpha_{R,l}(k) \triangleq \alpha_l e^{-j2\pi k \Delta f \tau_l} \mathbf{a}_T^T(\mu_{T,l})\mathbf{f}$ is a complex valued scalar. The vector $\mathbf{h}(k) \in \mathbb{C}^{N\times 1}$ is the effective complex channel vector at the receiver side on the k^{th} sub-carrier.

Note that equation (4) simplifies the model for the UE receive beam detection without the need to know the transmitter antenna size and the transmitter phase array setting at the BS side, which is practical for current cellular technologies such as 5G NR. We further apply the descrambling operation by multiplying with $s_m^*(k)$ on the k^{th} sub-carrier and stack the descrambled signal for all M measurements together. Then we get the measurement vector in the beamspace:

$$\begin{bmatrix} y_1(k)s_1^*(k) \\ \cdots \\ y_M(k)s_M^*(k) \end{bmatrix} = \begin{bmatrix} \mathbf{w}_1^H \\ \cdots \\ \mathbf{w}_M^H \end{bmatrix} \mathbf{h}(k) + \begin{bmatrix} \mathbf{w}_1^H \mathbf{z}_1(k) s_1^*(k) \\ \cdots \\ \mathbf{w}_M^H \mathbf{z}_M(k) s_M^*(k) \end{bmatrix} \tag{6}$$

which could be written in the compact form as:

$$\mathbf{y}(k) = \mathbf{W}^H \mathbf{h}(k) + \tilde{\mathbf{z}}(k), \;\; k \in 1, \ldots, K \tag{7}$$

where $\mathbf{y}(k) \in \mathbb{C}^{M\times 1}$ is the stacked measurement vector on the k^{th} sub-carrier for all M measurements, $\mathbf{W} \in \mathbb{C}^{N\times M}$ is the analog codebook for UE receive beam training, which is also denoted as the projection matrix, and $\tilde{\mathbf{z}}(k) \in \mathbb{C}^{M\times 1}$ is the modulated noise vector.

B. Receiver Beam Detection

We define $\mathbf{U} = [\ \mathbf{u}_1, \ldots, \mathbf{u}_P\ ] \in \mathbb{C}^{N\times P}$ as the analog codebook for UE communication, which has P candidate communication beams and $\mathbf{u}_i \in \mathbb{C}^{N\times 1}$ denotes the i^{th} codeword which corresponds to the i^{th} candidate communication beam. Note that $\mathbf{U}$ is distinct from the beam training analog codebook $\mathbf{W}$. In the same way as $\mathbf{W}$, $\mathbf{U}$ also has unit modulus entries.

In the receiver beam training phase, our objective is to detect the beam index $i^{(opt)}$ of the communication beam which maximizes the receive beamforming gain. The objective function for receive beam index detection can be defined as:

$$i^{(opt)} = \underset{i \in \{1,\dots,P\}}{\arg\max} \; \{\mathbf{u}_i^H \mathbf{R}_{hh} \mathbf{u}_i\} = \underset{i \in \{1,\dots,P\}}{\arg\max} \{g_i\} \tag{8}$$

where $\mathbf{R}_{hh} \in \mathbb{C}^{N \times N}$ is the wideband antenna element space covariance matrix (AESC). It is given by

$$\mathbf{R}_{hh} = \frac{1}{K} \sum_{k=0}^{K-1} \mathbf{h}(k)\mathbf{h}(k)^H \tag{9}$$

and g_i denotes the beamforming (BF) gain of the i^{th} communication beam candidate. It is worthwhile to mention that the objective function can also be modified based on the FB averaged version of $\mathbf{R}_{hh}$ [11],[12]

$$i^{(opt)} = \underset{i \in \{1,\dots,P\}}{\arg\max} \; \{\mathbf{u}_i^H \mathbf{R}_{hh}^{\mathrm{FB}} \mathbf{u}_i\} \tag{10}$$

where FB averaging is defined as:

$$\mathbf{R}_{hh}^{\mathrm{FB}} = \frac{1}{2}(\mathbf{\Pi}_N \mathbf{R}_{hh}^* \mathbf{\Pi}_N \; + \mathbf{R}_{hh}) \tag{11}$$

and $\mathbf{\Pi}_N$ is $N \times N$ anti-diagonal row-exchange matrix with ones on its anti-diagonal and zeros elsewhere. Meanwhile, for the measured signal, a wideband beamspace covariance matrix (BSC) can be derived as:

$$\mathbf{R}_{yy} = \frac{1}{K} \sum_{k=0}^{K-1} \mathbf{y}(k)\mathbf{y}(k)^H \tag{12}$$

Using (7) and (9), we rewrite (12) as

$$\begin{aligned} \mathbf{R}_{yy} =& \mathbf{W}^H \mathbf{R}_{hh} \mathbf{W} + \frac{\sigma^2}{K} \mathbf{W}^H \mathbf{W} \\ =& \tilde{\mathbf{R}}_{yy} + \frac{\sigma^2}{K} \mathbf{W}^H \mathbf{W} \end{aligned} \tag{13}$$

where $\tilde{\mathbf{R}}_{yy} \triangleq \mathbf{W}^H \mathbf{R}_{hh} \mathbf{W}$. The matrix $\mathbf{R}_{yy}$ can be viewed as a noisy compressed feature set which is projected from $\mathbf{R}_{hh}$, while $\mathbf{R}_{hh}$ is further linked to the best UE communication beam. With that in mind, instead of first applying compressive recovery of $\mathbf{R}_{hh}$ from $\mathbf{R}_{yy}$ and then computing the BF gains of all communication beam candidates, we propose to make use of a simple feed-forward NN to directly predict the BF gains based on $\mathbf{R}_{yy}$. Also, we propose that, with proper design of the training beam codebook $\mathbf{W}$, the real part of $\mathbf{R}_{yy}$ is equivalent to the noisy projected version of $\mathbf{R}_{hh}^{\mathrm{FB}}$. Using only the real part of $\mathbf{R}_{yy}$ leads to further input feature compression such that a NN with less number of nodes can be used to detect the best beam without accuracy loss. In the next section we describe the design of the NN and the projection matrix $\mathbf{W}$ in detail.

III. Proposed Approach

A. Projection Matrix Design

In this section, we present the design of the projection matrix $\mathbf{W}$ which enables real-valued beamspace covariance processing. Based on the theory in [13], assume that $\mathbf{Q} \in \mathbb{C}^{N \times M}$ is any column conjugate symmetric matrix, i.e.,

$$\mathbf{\Pi}_N \mathbf{Q} = \mathbf{Q}^*, \tag{14}$$

then, any centro-Hermitian matrix $\mathbf{R} \in \mathbb{C}^{N \times N}$ could be mapped to a real-valued matrix $\tilde{\mathbf{R}} \in \mathbb{R}^{M \times M}$ as follows:

$$\tilde{\mathbf{R}} = \mathbf{Q}^H \mathbf{R} \mathbf{Q} \tag{15}$$

For our application, to ensure the centro-Hermitian property, we replace $\mathbf{R}$ by $\mathbf{R}_{hh}^{\mathrm{FB}}$ as defined in (11). Also, to satisfy the column conjugate symmetry, we replace $\mathbf{Q}$ by our projection matrix $\mathbf{W}$ with the following structure: If N is even,

$$\mathbf{W} = \begin{bmatrix} \mathbf{A} \\ \mathbf{\Pi}_{\frac{N}{2}} \mathbf{A}^* \end{bmatrix} \tag{16}$$

where $\mathbf{A} \in \mathbb{C}^{\lfloor \frac{N}{2} \rfloor \times M}$ is a random phase matrix following the constant modulus (CM) constraint of the analog beams. If N is odd,

$$\mathbf{W} = \begin{bmatrix} \mathbf{A} \\ \mathbf{r} \\ \mathbf{\Pi}_{\lfloor \frac{N}{2} \rfloor} \mathbf{A}^* \end{bmatrix} \tag{17}$$

where $\mathbf{r}$ is $1 \times M$ a row vector of unit modulus elements with random phases.

For the case where N is even, $\mathbf{W}$ can be proved to be column conjugate symmetric by substituting (16) in (14) while decomposing $\mathbf{\Pi}_N$ into a $\frac{N}{2} \times \frac{N}{2}$ sub-structure as follows:

$$\mathbf{\Pi}_N \mathbf{W} = \begin{bmatrix} \mathbf{0} & \mathbf{\Pi}_{\frac{N}{2}} \\ \mathbf{\Pi}_{\frac{N}{2}} & \mathbf{0} \end{bmatrix} \begin{bmatrix} \mathbf{A} \\ \mathbf{\Pi}_{\frac{N}{2}} \mathbf{A}^* \end{bmatrix} = \begin{bmatrix} \mathbf{A}^* \\ \mathbf{\Pi}_{\frac{N}{2}} \mathbf{A} \end{bmatrix} = \mathbf{W}^* \tag{18}$$

where $\mathbf{0}$ denotes the $\frac{N}{2} \times \frac{N}{2}$ matrix of all zeros and we used the fact that $\mathbf{\Pi}_{\frac{N}{2}} \mathbf{\Pi}_{\frac{N}{2}} = \mathbf{I}_{\frac{N}{2}}$. A similar proof holds if N is odd.

Replacing $\mathbf{R}$ by $\mathbf{R}_{hh}^{\mathrm{FB}}$ and $\mathbf{Q}$ by $\mathbf{W}$ in (15) and using the properties in (14), we get:

$$\begin{aligned} \tilde{\mathbf{R}} =& \mathbf{W}^H \mathbf{R}_{hh}^{\mathrm{FB}} \mathbf{W} \\ =& \frac{1}{2}(\mathbf{W}^H \mathbf{\Pi}_N \mathbf{R}_{hh}^* \mathbf{\Pi}_N \mathbf{W} + \mathbf{W}^H \mathbf{R}_{hh} \mathbf{W}) \\ =& \frac{1}{2}(\mathbf{W}^T \mathbf{R}_{hh}^* \mathbf{W}^* + \mathbf{W}^H \mathbf{R}_{hh} \mathbf{W}) \\ =& \Re\{\mathbf{W}^H \mathbf{R}_{hh} \mathbf{W}\} \\ =& \Re\{\tilde{\mathbf{R}}_{yy}\} \end{aligned} \tag{19}$$

Equations (19) and (13) show that, by designing the projection matrix $\mathbf{W}$ to be structured random and column conjugate symmetric, the real part of $\mathbf{R}_{yy}$ corresponds to the noisy compressive projection of $\mathbf{R}_{hh}^{\mathrm{FB}}$, which is the FB averaged version of $\mathbf{R}_{hh}$.

B. Neural Network Design

In this section, we present the design of the NN which directly predicts the BF gain vector for all P candidate communication beams, $\hat{\mathbf{g}} = [\hat{g}_1, \ldots, \hat{g_P}]$, based on $\mathbf{R}_{yy}$. The NN is based on a multi-output regression model and is further shown in Fig.1, which consists of 1 input layer, 2 hidden layers with ReLu activation functions, and 1 output layer with linear activation functions. All layers are fully connected. The number of nodes per layer is N_f, $4N_f$, $2N_f$ and P, respectively, where N_f is the number of input features. By considering that $\mathbf{R}_{yy}$ is a Hermitian matrix, only the upper or lower triangular elements of $\mathbf{R}_{yy}$ are needed. Furthermore, two variants are explored: The first variant is to stack the real and imaginary parts of the non-diagonal upper triangular elements, plus the real parts of the diagonal elements of $\mathbf{R}_{yy}$ as the input feature vector into the NN. This results in $N_f = M^2$. We denote this variant as Beamspace Covariance NN (BSC-NN). The second variant considers the property of (19), so that only the real parts of the upper triangular elements of $\mathbf{R}_{yy}$ are stacked as the input feature vector. In this case $N_f = \frac{1}{2}M(M+1)$. We denote this variant as Real-valued Beamspace Covariance NN (RBSC-NN). We can see that the number of nodes and interconnections of RBSC-NN is much smaller than that of BSC-NN.

Both NNs are trained in a supervised manner. The cost function used for training is defined as follows:

$$L_{MSE} = \frac{1}{S}\sum_{s=1}^{S} \|\mathbf{g}^{(s)} - \hat{\mathbf{g}}^{(s)}\|^2 \tag{20}$$

where S is the total number of training samples. For the s^{th} training sample, $\mathbf{g}^{(s)}$ is the ideal BF gain vector calculated based on the perfect knowledge of $\mathbf{R}_{hh}$, and $\hat{\mathbf{g}}^{(s)}$ is the NN predicted BF gain vector based on $\mathbf{R}_{yy}$.

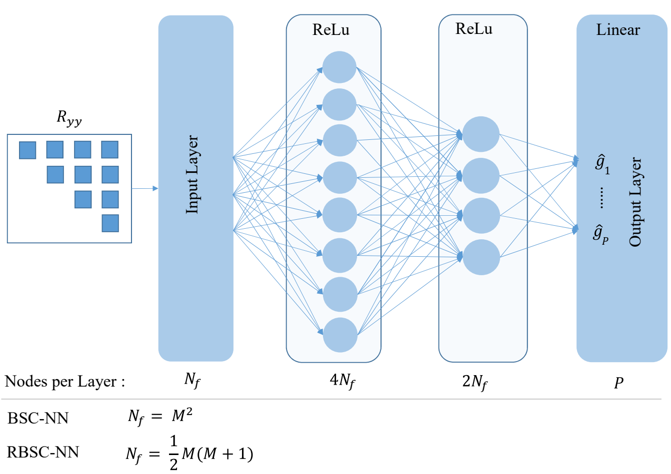

Fig. 1: Proposed Neural Network Structure

IV. Simulation Results

We evaluate the performance of our proposed BSC-NN and RBSC-NN using 3GPP defined Clustered-Delay Line (CDL) channel models [14]. Both the line-of-sight (LOS) scenario using the CDL-D profile and the non-line-of-sight (NLOS) scenario using the CDL-A profile are examined. Table I summarizes the simulation parameters. The designed NNs are trained using Tensorflow with 6000 epochs and the batch size is set to 600 every epoch. We use the Adam optimizer with zero regularization loss and the learning rate is set to be 0.001. The training and validation data were randomly generated using the parameters in Table I at 20dB SNR and the sizes of the training and validation sets were 5000 and 500 samples, respectively. For the testing, we generated data sets in the SNR range from -6 to 12 dB. At each SNR point we generated 2000 data points where the azimuth angle of arrival (AoA) was randomly generated from $[-\frac{\pi}{2}, \ldots, \frac{\pi}{2}]$. The beam training codebook $\mathbf{W}$ with structured random phases was generated according to the design in (16). The mutual coherence (MC) of the sensing matrix is further minimized by using the schemes described in [3]. The resulting beam patterns of the training codebook are shown in Fig.2. The communication codebook $\mathbf{U}$ is chosen as a DFT codebook with an oversampling factor of 2. The performance is evaluated by averaging the achieved receive BF gains over all Monte Carlo iterations at each SNR point. The comparisons are made with the case of perfect CSI in the antenna element space and with the state-of-the-art 2-step approach using the COMP algorithm [5].

Simulation parameters	**Values**
Carrier frequency	28 GHz
Sub-carrier spacing	120 KHz
Pilot signal type	BM CSI-RS
Num. of OFDMs within a beam training burst (M)	4
Num. of receive antennas (N)	8
Num. of UE communication beam candidates (P)	16

TABLE I: Simulation Parameters

For the LOS channel which is highly sparse, we see that all three algorithms approach the ideal curve with perfect CSI on most of the SNR points. It is interesting to observe that, although the proposed RBSC-NN has a lower complexity than the BSC-NN due to the real-valued beamspace processing, it achieves an even slightly better accuracy than the BSC-NN. That is mainly due to the improved neural network (NN) efficiency by using more compacted features. For the NLOS channel where the channel sparsity is reduced because of the increased number of strong reflection clusters as well as the angular spreads, NN based methods significantly outperform COMP for medium and high SNR regions. The gain is due to the fact that the optimization target of COMP is to minimize the errors for the $\mathbf{R}_{hh}$ recovery while the optimization target of the proposed NN based methods is to directly minimize the prediction error of the BF gains of the communication

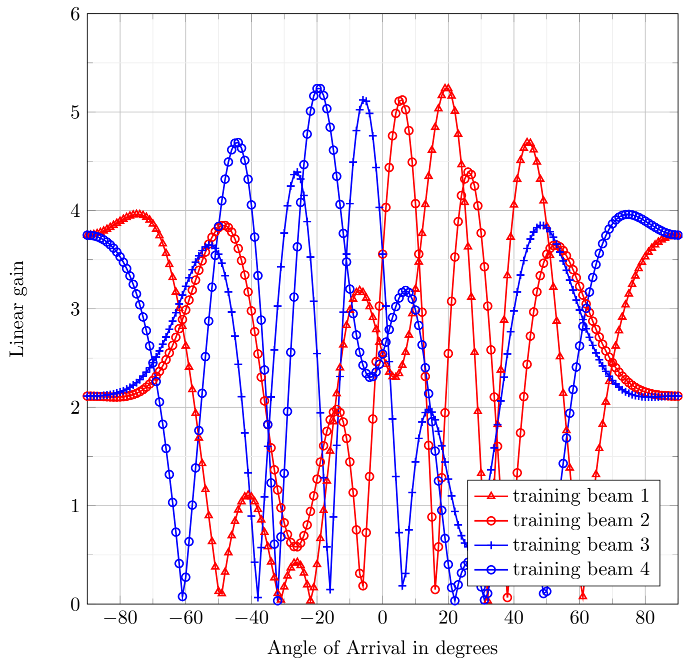

Fig. 2: Radiation pattern for the designed training beams

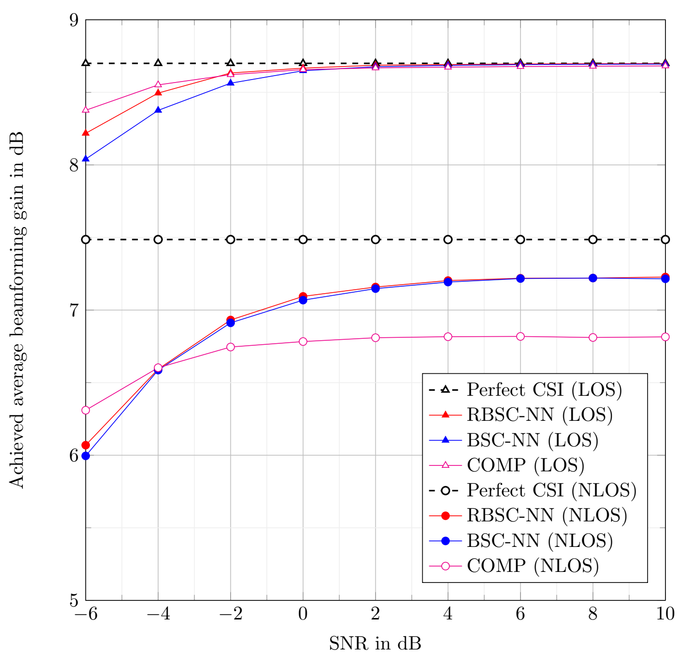

Fig. 3: Achieved BF gain versus SNR under 3GPP CDL channels

codebook, so that the grid-mismatch issues can be mitigated through learning. Note that for very low SNR regions, the NN based methods perform slightly worse than COMP. That is because so far the training samples are obtained under high SNR. However, by considering the fact that UE RX beam detection for the serving BS is usually operated at medium or high SNR, such a loss can be ignored in practice.

V. Conclusions

This paper presents a learning based compressive beam detection scheme using the spatial channel covariance matrix in beamspace. By introducing structured random training beams which are conjugate symmetric, the real part of the upper triangular elements of the beamspace spatial channel covariance matrix can be viewed as the compressed features for communication beam detection. Thus only a tiny real-valued NN is required, which can be easily implemented in a mobile terminal device with low complexity. Simulations show that the proposed scheme can detect the best communication beam with high accuracy using only a few measurements. For future work we are going to extend the scheme to be robust against phase errors as well as beam squint. We also plan to evaluate the scheme for larger antenna arrays.

References

[1] R. W. Heath, N. González-Prelcic, S. Rangan, W. Roh, and A. M. Sayeed, “An overview of signal processing techniques for millimeter wave MIMO systems,” *IEEE Journal of Selected Topics in Signal Processing*, vol. 10, no. 3, pp. 436–453, 2016.

[2] J. Rodríguez-Fernández, N. González-Prelcic, K. Venugopal, and R. W. Heath, “Frequency-domain compressive channel estimation for frequency-selective hybrid millimeter wave MIMO systems,” *IEEE Transactions on Wireless Communications*, vol. 17, no. 5, pp. 2946–2960, 2018.

[3] K. Ardah and M. Haardt, “Compressed sensing constant modulus constrained projection matrix design and high-resolution DoA estimation methods,” in *Proc. 25th International ITG Workshop on Smart Antennas (WSA)*, 2021, pp. 1–5.

[4] N. J. Myers and R. W. Heath, “Localized random sampling for robust compressive beam alignment,” in *Proc. IEEE International Conference on Acoustics, Speech and Signal Processing (ICASSP)*, 2019, pp. 4644–4648.

[5] S. Park and R. W. Heath, “Spatial channel covariance estimation for the hybrid MIMO architecture: A compressive sensing-based approach,” *IEEE Transactions on Wireless Communications*, vol. 17, no. 12, pp. 8047–8062, 2018.

[6] W. Ma, C. Qi, and G. Y. Li, “Machine learning for beam alignment in millimeter wave massive MIMO,” *IEEE Wireless Communications Letters*, vol. 9, no. 6, pp. 875–878, 2020.

[7] X. Li and A. Alkhateeb, “Deep learning for direct hybrid precoding in millimeter wave massive MIMO systems,” in *Proc. 53rd Asilomar Conference on Signals, Systems, and Computers*, 2019, pp. 800–805.

[8] H. Yan, B. W. Domae, and D. Cabric, “MmRAPID: Machine learning assisted noncoherent compressive millimeter-wave beam alignment,” in *Proc. 4th ACM Workshop on Millimeter-Wave Networks and Sensing Systems*, ser. mmNets’20. New York, NY, USA: Association for Computing Machinery, 2020.

[9] J. Zhang, H. Wang, G. Du, and H. Xie, “Deep learning for fast beam tracking using RSRP in millimeter wave MIMO systems,” in *Proc. IEEE 95th Vehicular Technology Conference: (VTC2022-Spring)*, 2022, pp. 1–5.

[10] J. Zhang and M. Haardt, “Channel estimation and training design for hybrid multi-carrier mmwave massive MIMO systems: The beamspace ESPRIT approach,” in *Proc. 25th European Signal Processing Conference (EUSIPCO)*, 2017, pp. 385–389.

[11] M. Pesavento, A. Gershman, and M. Haardt, “Unitary root-MUSIC with a real-valued eigendecomposition: a theoretical and experimental performance study,” *IEEE Transactions on Signal Processing*, vol. 48, no. 5, pp. 1306–1314, 2000.

[12] A. Gershman and P. Stoica, “On unitary and forward–backward MODE,” *Digital Signal Processing*, vol. 9, no. 2, pp. 67–75, 1999.

[13] A. Lee, “Centrohermitian and skew-centrohermitian matrices,” *Linear Algebra and its Applications*, vol. 29, pp. 205–210, 1980.

[14] TR 38.901, “Study on channel model for frequencies from 0.5 to 100 GHz,” 3rd Generation Partnership Project (3GPP), Technical Report (TR) 38.901, 03 2022, version 17.0.0. [Online]. Available: https://portal.3gpp.org